CERAMIC RELIABILITY FOR MICROTURBINE HOT-SECTION COMPONENTS

Reliability Evaluation of Microturbine Components

H. T. Lin, M. K. Ferber, and T. P. Kirkland
Oak Ridge National Laboratory
Oak Ridge, TN 37831-6068
Phone: (865) 576-8857, E-mail: linh@ornl.gov

Objective

Evaluate and document the long-term mechanical properties of very small specimens machined from ceramic components (e.g., blades, nozzles, vanes, and rotors) in as processed and after engine testing at ambient and elevated temperatures under various controlled environments. This work will allow microturbine companies to verify mechanical properties of components and apply the generated database in probabilistic component design and lifetime prediction methodologies. The work also provides a critical insight into how the microturbine environments influence the microstructure and chemistry, thus mechanical performance of materials.

Highlights

Studies of mechanical properties of biaxial discs machined from airfoils of SN282 silicon nitride integral vane ring (Kyocera Industrial Ceramic Corp., Vancouver, WA) was completed. The SN282 silicon nitride integral vane ring, acquired from UTRC, was designed for UTRC ST5+ advanced microturbine system (Fig. 1). Biaxial discs (7 mm in diameter x 0.5 mm in thickness) were machined from airfoils. Ball-on-ring test was carried out at room temperature with the as-processed surface under tension. Database generated has been provided to Kyocera for processing refinement, and also to UTRC for its probabilistic component design and life prediction effort.

Figure 1. Photos of UTRC SN282 silicon nitride integral vane ring designed for ST5+ advanced microturbine system.

Development and Characterization of Advanced Materials for Microturbine Applications

M. K. Ferber and H-T Lin
Metals and Ceramics Division
Oak Ridge National Laboratory
P.O. Box 2008, Oak Ridge, TN 37831-6069
Phone: (865) 576-0818, E-mail: ferberk@ornl.gov

Objective

The primary objective of this project is to evaluate the long-term mechanical and chemical stability of advanced materials of interest to the DER program. Currently the project is evaluating (1) structural ceramic, which are being considered for use as hot-section components in microturbines and (2) thick thermal barrier coatings (TTBCs) being developed for thermal management in combustor liners used in industrial gas turbines. The structural ceramics effort focuses on the development and utilization of test facilities for evaluating the influence of high-pressure and high-temperature water vapor upon the long-term mechanical behavior of monolithic ceramics having environmental barrier coatings. In the case of the TTBCs, the primary focus is on the evaluation of changes in microstructure and thermal properties arising from long-term aging tests.

A secondary objective of the program is to develop and characterize the toughened silicon nitride ceramics with the following attributes:

- Fracture toughness $\geq$ 10 MPa•$m^{1/2}$ with fracture strengths > 1 GPa, and
- High mechanical reliability at low and intermediate temperatures coupled with creep resistance at the desired operating temperatures,
- Enhanced resistance to elevated temperature environmental damage, and
- Higher thermal expansion coefficients to better match the expansion of promising environmental barrier coating (EBC) systems.

Highlights

A program to graphically illustrate component reliability for selected structural ceramics was developed. This program utilizes strength/stress versus temperature plots to compare finite element results for a specific component with the strength-temperature data for a number of commercial silicon nitride ceramics. The strength is adjusted to account for both slow crack growth and creep. The effect of recession is simulated by increasing the finite element stresses as the material is lost.

Technical Progress

The steam injection system (Figure 1) described in the previous quarterly report was used to evaluate the temperature sensitivity of recession of the SN282 silicon nitride by exposing three specimens at 1100, 1200, and 1300°C. The recession was evaluated as a function of time by

interrupting each test periodically and measuring the change in the gage diameter using a coordinate measuring machine. The maximum loss in gage diameter was taken as the appropriate measure of surface recession. The mid-span profiles of the specimens exposed for 884 h are shown in Figure 2. These data were subsequently used to calculate recession as a function of angle measured with respect to the injection direction (Figure 3). Although the maximum reduction in gage diameter for the specimen exposed at 1200°C was slightly larger than that at 1300°C, the total amount of material loss was much larger for the specimen exposed at 1300°C. The recession of the 1300°C specimen was also more asymmetric in that the recession along one side (angle = 90°) was much greater than that along the opposing side. These differences were attributed to variability in the geometries of the alumina injection tubes. As shown in Figure 4, the gap of the injection tube used with the specimen exposed at 1200°C was very well matched to the gage diameter (6.35 mm). In the case of the injection tube used with the specimen exposed at 1300°C, the gap (6.98 mm) was significantly larger that the gage diameter indicating that it was less effective at restricting the steam flow. One would expect that the local velocity would be smaller for this case.

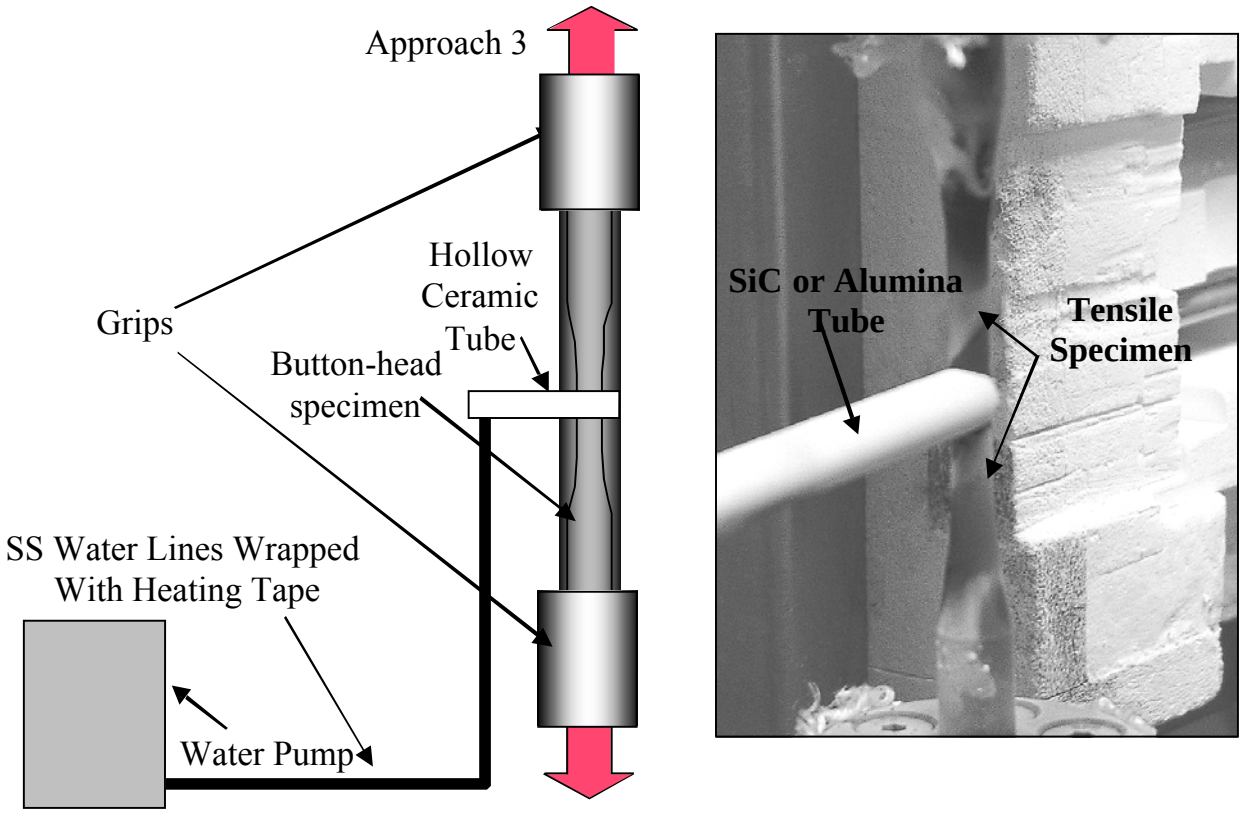

Figure 1: Direct Steam Injection System.

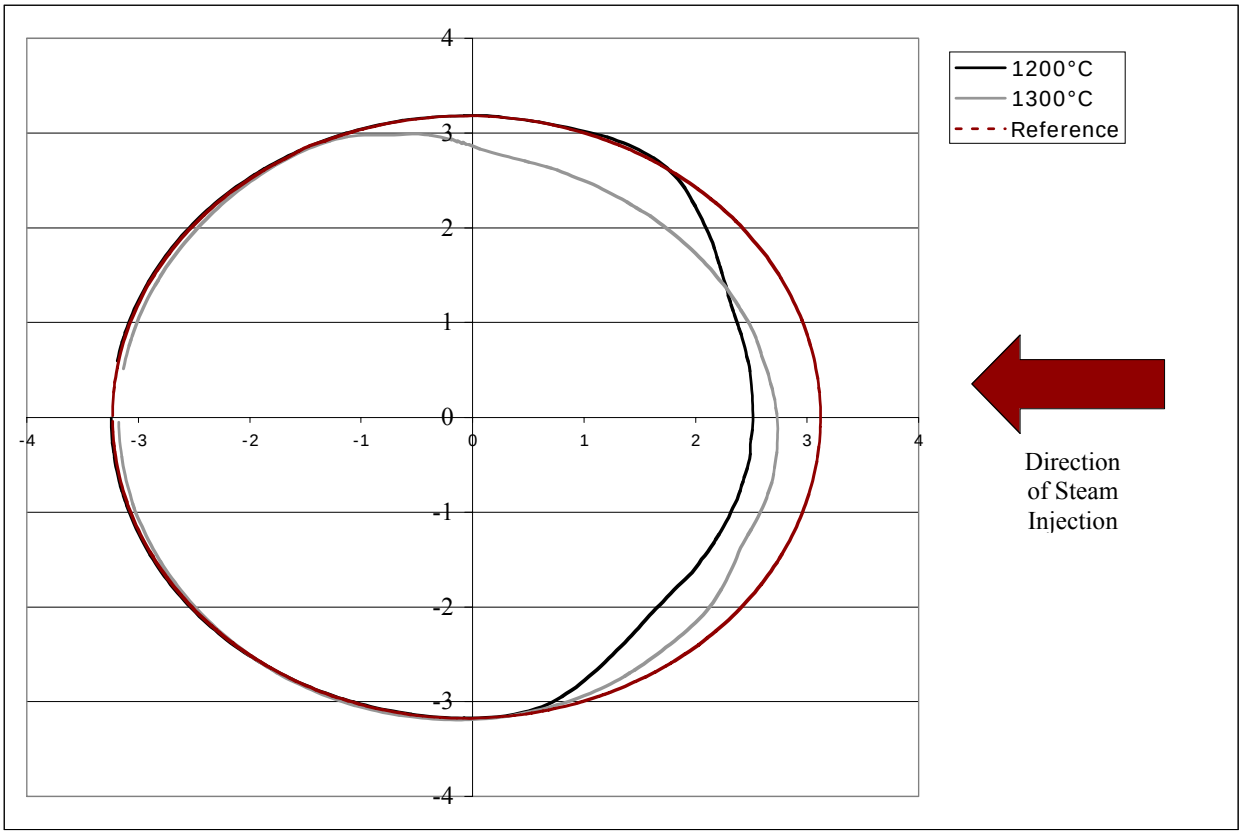

Figure 2: Surface profiles for specimens exposed at 1200 and 1300°C.

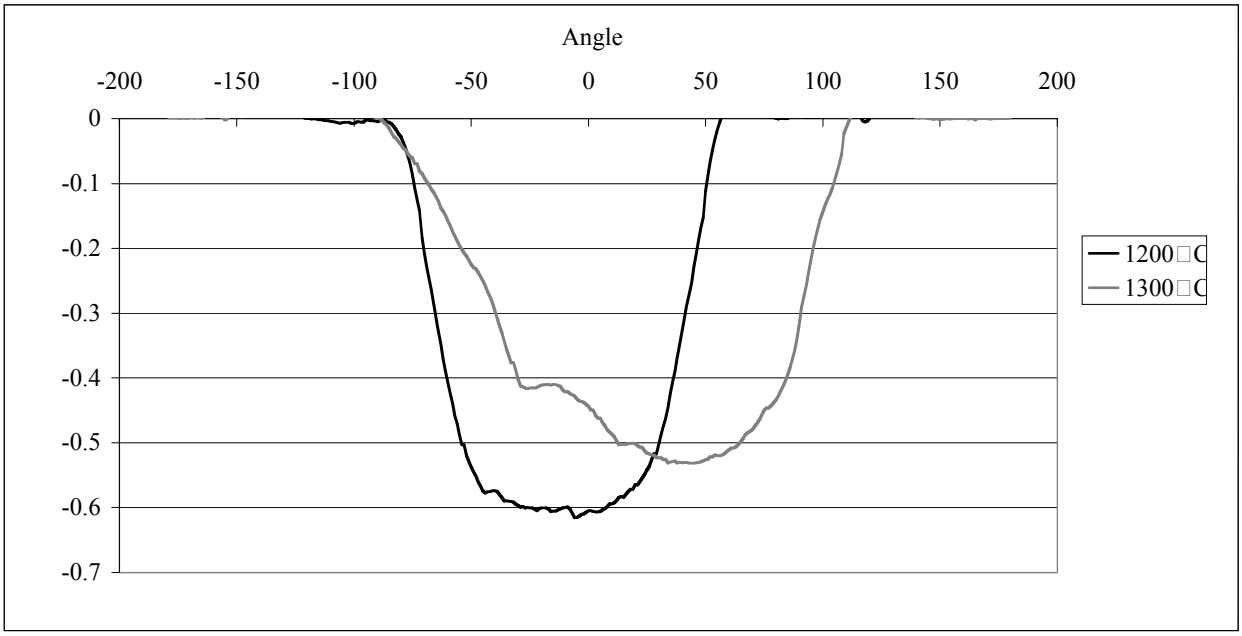

Figure 3: Extent of recession as a function of angle measured with respect injection direction.

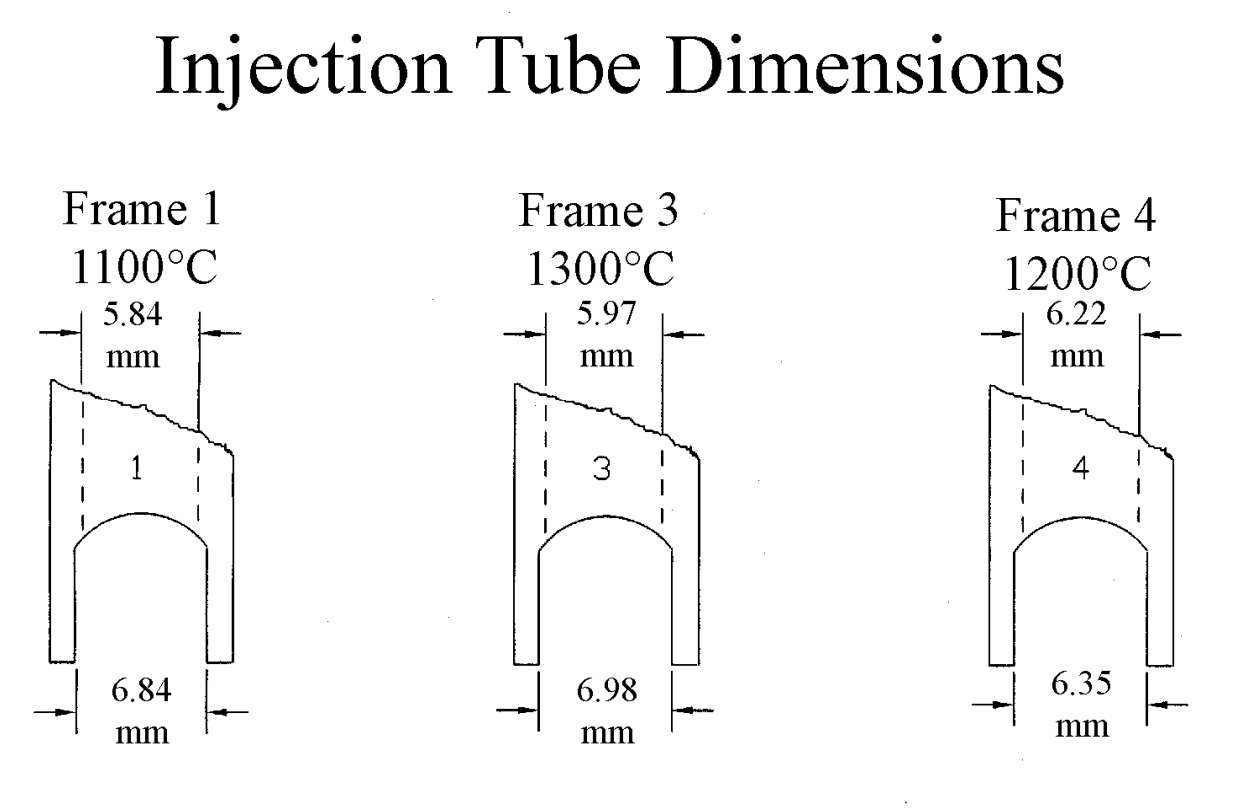

Figure 4: Geometry of the alumina injection tubes.

Status of Milestones

(1) Complete the characterization of thick thermal barrier coatings (supplied by Solar Turbines) aged for periods up to 5000 and issue report-March 2004 Completed

(2) Complete mechanical property assessment of toughened silicon nitride ceramics and incorporate into database-October 2004

(3) Complete the characterization of commercially available environmental barrier coatings and issue report-March 2005.

Industry Interactions

Teleconferences were held Jay Morrison of Siemens to discuss the characterization of their alumina composites and thermal barrier coatings.

Problems Encountered

None

Publications

None

References

None

Technical Progress

Studies of dynamic fatigue properties for SiAlON ceramics (Kennametal Inc., PA) were continued during this reporting period. Kennametal was awarded by DOE under Microturbine Materials Program to develop SiAlON ceramics for hot-section components for advanced microturbines. The SiAlON ceramics due to their superior wear resistance have been developed for metal cutting tool applications, and might have great potential for structural applications in microturbine systems. The purpose of this study is to generate a database for down-selecting the candidate composition(s) and also for probabilistic component design and life prediction efforts carried out by microturbine companies. All of the materials, sintered with different chemical compositions, i.e., rare earth oxide content, contain a mixture of α- and β-SiAlON grain microstructure. The SiAlON ceramics were fabricated under the Phase I contract, and MOR bars were longitudinally machined per the revised ASTM C116 standard with 600 grit surface finish. The dynamic fatigue tests were carried out at 20 and 1204°C and at stressing rate of 30 and 0.003 MPa/s in air per ASTM C1465. The 30 MPa/s is used to evaluate the inert characteristic strength as a function of temperature, and 0.003 MPa/s is applied to measure the slow crack growth (SCG) susceptibility at high temperatures.

Test results at 20°C and 30 MPa/s showed that all of the SiAlON materials exhibited comparable relatively low Weibull modulus with respect to commercially available silicon nitride ceramics evaluated and reported previously (Table 1 and Fig. 2-7). Preliminary fractography examinations indicated the low Weibull moduli obtained for all of the SiAlON materials evaluated might result from the metal contamination during processing. Also, results showed that the values of the inert characteristic strength of SiAlON strongly depended on the size and content of elongated β-SiAlON grains. For instance, the material contained fine α-SiAlON matrix plus a relative high content of β-SiAlON grains (e.g., AB832 and AB832) exhibited higher characteristic strengths than those with more equiaxed microstructure (e.g., AB582 and AB532). The effect of β-SiAlON elongated grain size and content on the measured mechanical strength is consistent with those previously reported for silicon nitride ceramics. On the other hand, results showed there was minor change in inert characteristic strength accompanied with a high fatigue exponent for 2308E material when tested at 20°C and 0.003 MPa/s (Fig. 8 and 9). Note that the 2308E material showed a 20% degradation in strength with a low fatigue exponent (~36) when tested at 1204°C (Table 1), indicative of high susceptibility to SCG at temperature. Dynamic fatigue tests at 1204°C will be carried out for these SiAlON materials and results will be discussed in the next quarterly report.

Table 1. Summary of uncensored Weibull and strength distributions for Kennametal SiAlON ceramic specimens with as-machined surface (longitudinally machined per the revised ASTM C1161 standard).

Material	# of Spmns. Tested	Stressing Rate (MPa/s)	Temp. (°C)	Uncens. Weibull Modulus	± 95% Uncens. Weibull Modulus	Uncens. Chrctstic Strength (MPa)	± 95% Uncens. Chrctstic Strength (MPa)
2308A	15	30	20	5.92	3.80, 8.55	651	589, 715
2308E	15	30	20	6.06	3.91, 8.73	783	710, 858
2308E	12	0.003	20	6.62	4.06, 9.90	807	729, 887
AB132	15	30	20	6.39	4.16, 9.14	878	801, 958
AB531	15	30	20	10.65	6.75, 15.55	801	757, 844
AB532	15	30	20	8.47	5.27, 12.65	721	673, 771
AB582	15	30	20	7.21	4.65, 10.34	567	523, 613
AB831	15	30	20	8.45	5.42, 12.29	960	894, 1025
AB832	15	30	20	10.70	6.83, 15.57	1029	973, 1084
2308A	15	30	1204	9.79	6.52, 13.62	393	370, 415
2308E	15	30	1204	7.45	4.67, 11.05	540	489, 582
2308A	15	0.003	1204	10.68	6.87, 15.38	415	392, 437
2308E	14	0.003	1204	3.37	2.29, 4.55	440	369, 522

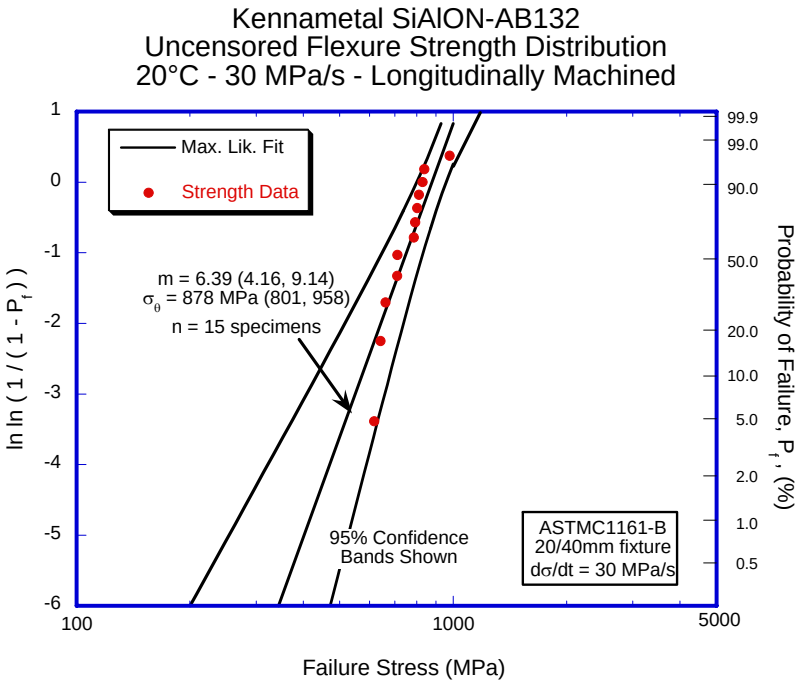

Figure 2. Uncensored flexure strength distribution at 20°C and 30 MPa/s of SiAlON-AB132 ceramic with as-machined surface (bulk material).

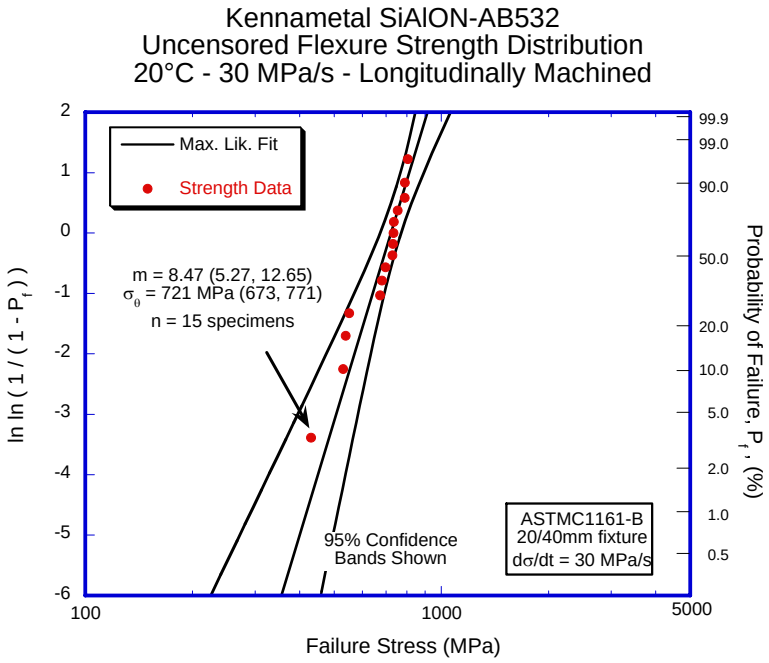

Figure 3. Uncensored flexure strength distribution at 20°C and 30 MPa/s of SiAlON-AB531 ceramic with as-machined surface (bulk material).

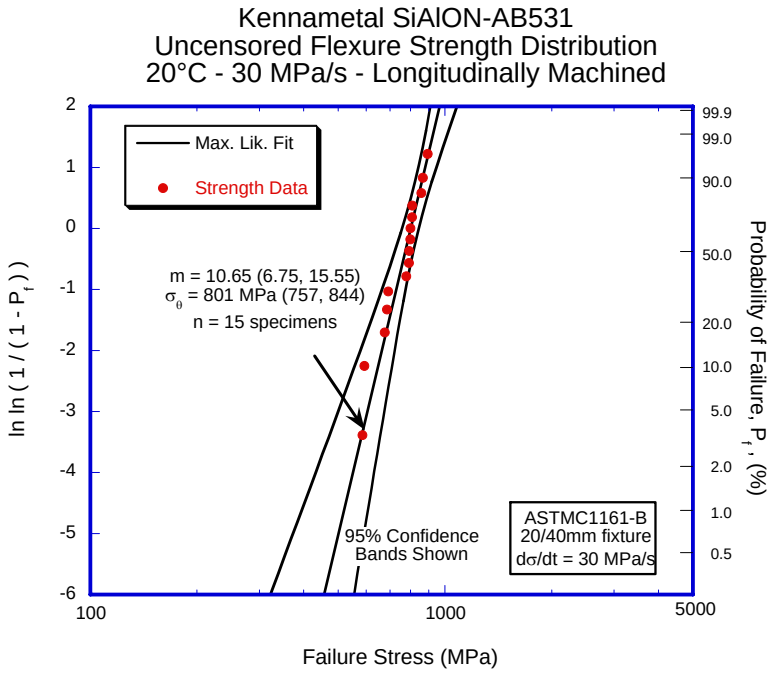

Figure 4. Uncensored flexure strength distribution at 20°C and 30 MPa/s of SiAlON-AB532 ceramic with as-machined surface (bulk material).

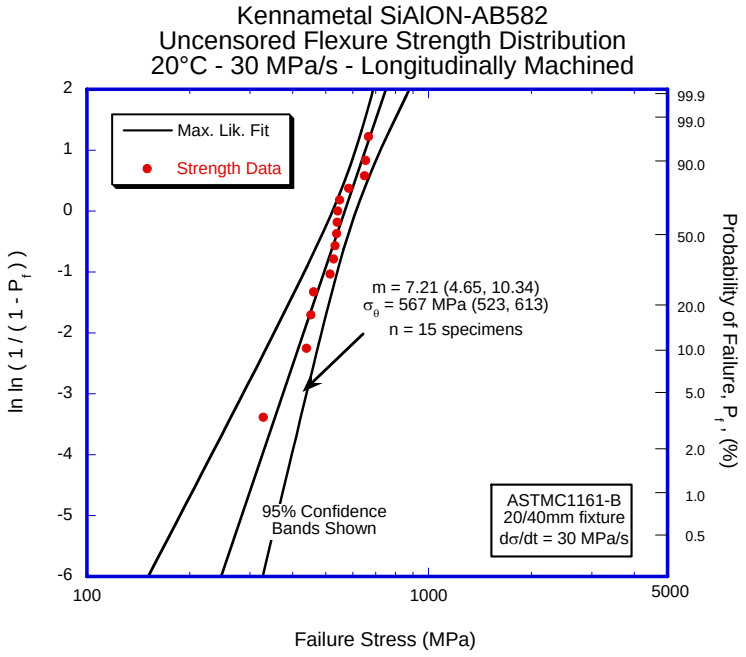

Figure 5. Uncensored flexure strength distribution at 1204°C and 30 MPa/s of SiAlON-AB582 ceramic with as-machined surface (bulk material).

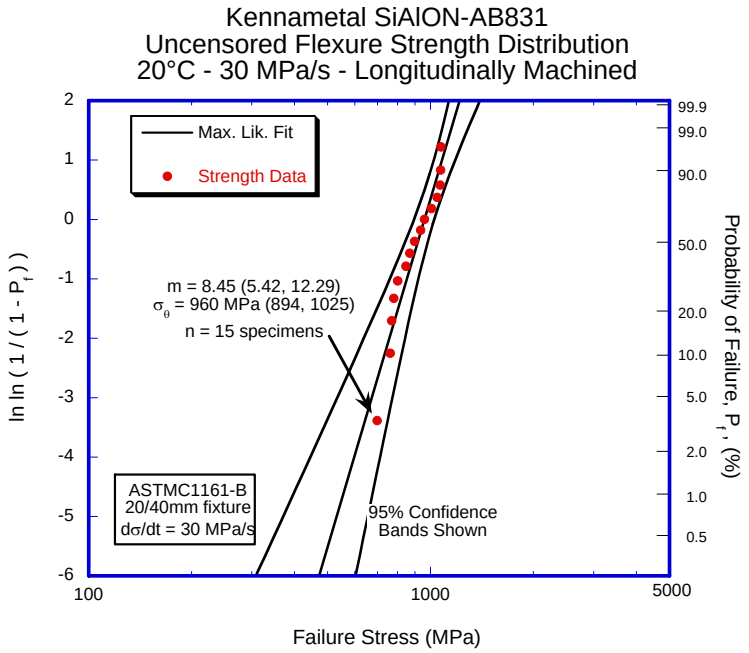

Figure 6. Uncensored flexure strength distribution at 1204°C and 30 MPa/s of SiAlON-AB831 ceramic with as-machined surface (bulk material).

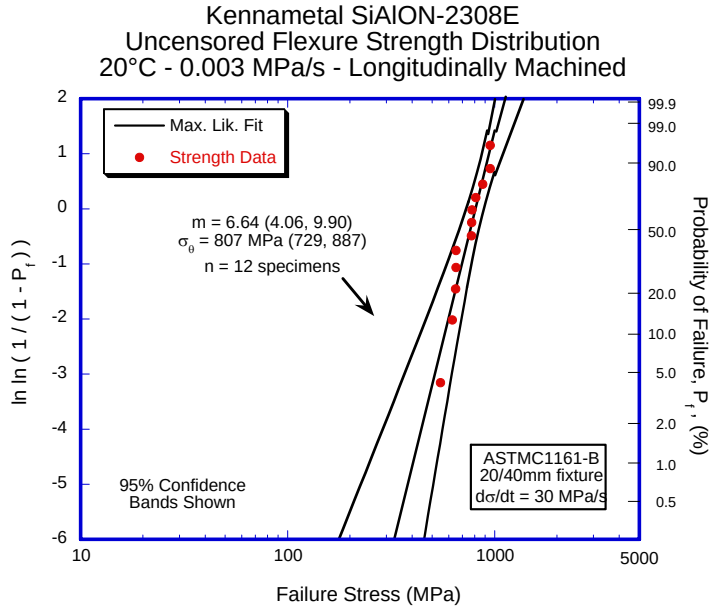

Figure 7. Uncensored flexure strength distribution at 20°C and 30 MPa/s of SiAlON-AB832 ceramic with as-machined surface (bulk material).

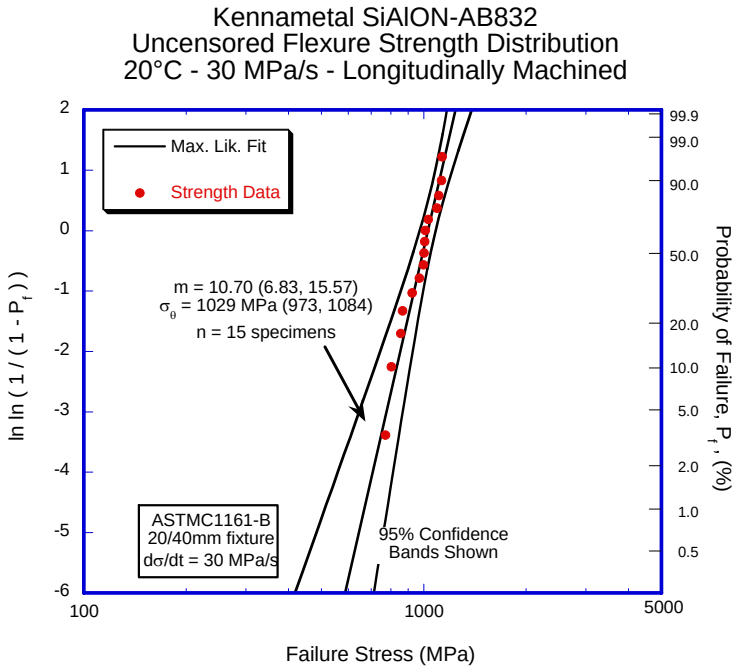

Figure 8. Uncensored flexure strength distribution at 20°C and 0.003 MPa/s of SiAlON-2308E ceramic with as-machined surface (bulk material).

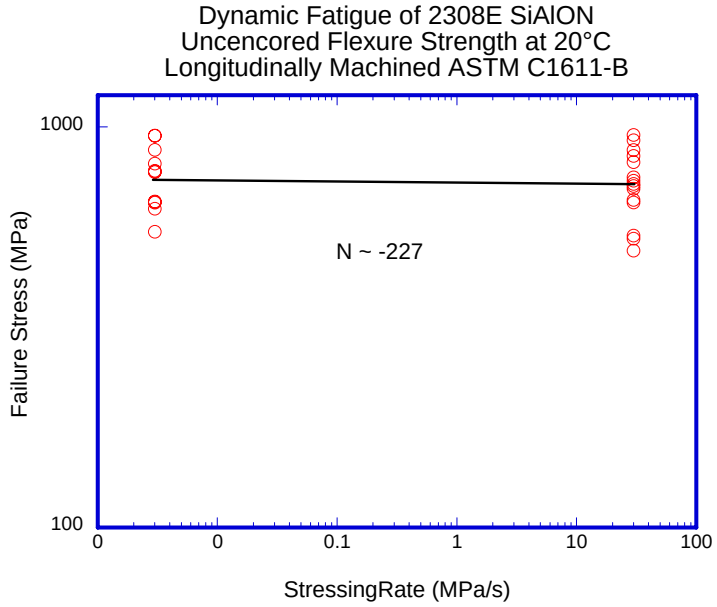

Figure 9. Flexure strength versus stressing rate for SiAlON-2308E with as-machined surface (bulk material) tested at 20°C.

An Ingersoll-Rand type NT154 silicon nitride microturbine rotor, similar to Kyocera SN237 rotor, has been received from Saint-Gobain Ceramics & Plastics (Fig. 10). Biaxial discs will be machined from airfoils for mechanical strength evaluation using

ball-on-ring method at room temperature. Test results will be provided to Saint-Gobain for processing optimization and to microturbine companies for their probabilistic component design and life prediction.

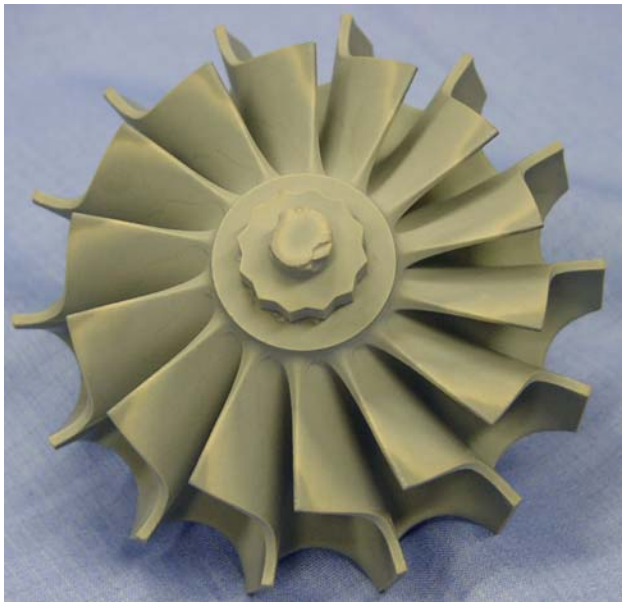

Figure 10. Photo of NT154 silicon nitride microturbine rotor manufactured by Saint-Gobain.

Status of Milestones

1. Complete evaluation of next generation Si_3N_4 with EBC from SMRC, Japan after long-term steam jet testing. September 2004. On schedule.

Industry Interactions

Communication with John Holowczak, Venkata Vedula, and Jun Shih at UTRC to discuss the mechanical results of SN282 integral vane ring.

Communication with Vimal Pujari and Ara Vartabedian at Saint-Gobain Ceramics & Plastics on the updates of the testing status and results for NT154 silicon nitride materials manufactured during Task II effort under Phase I contract, and also the preparation status for NT154 microturbine rotor.

Communication with Russ Yeckley at Kennemetal on the dynamic fatigue test results of SiAlON ceramics manufactured during Task I effort.

Communication with Professor Rishi Raj at University of Colorado on the testing and evaluation of SiCN EBC materials under steam environments.

Problems Encountered

None

Publications/Presentations

H. T. Lin and M. K. Ferber, "Evaluation Methodology for Mechanical Property of Complex-Shaped Ceramic Components." Presented at International Cocoa Beach Conference & Exposition on Advanced Ceramics & Composites, Cocoa Beach, FL, January 25-30, 2004

M. K. Ferber, H. T. Lin, S. F. Duffy, J. K. Kesseli, and M. Costen, "Characterization of a Ceramic Rotor Developed for the IR Power Works Microturbine," Presented at International Cocoa Beach Conference & Exposition on Advanced Ceramics & Composites, Cocoa Beach, FL, January 25-30, 2004.

Reliability Analysis of Microturbine Components

S.F. Duffy, E.H. Baker & J.L. Palko
Connecticut Reserve Technologies, LLC
2997 Sussex Court
Stow, Ohio 44224
Phone: 330-678-7328 E-mail: sduffy@crtechnologies.com

Objective

The current objectives of this project are as follows:

- Connecticut Reserve Technologies, LLC (CRT) will create the ability whereby an end user generates output in the form of unitless area- or volume- (or both) loading factors (k_A and k_V, respectively) as a function of Weibull modulus. Additional output will include the discrete area and volume that are used in the calculation of effective areas and effective volumes (i.e., report 6 values: k_A, k_V, A, V, $k_A \bullet A$, and $k_V \bullet V$). This will allow users of the software to conduct nonstandard parameter estimation analyses assuming the existence of either surface flaw populations, volume flaw populations, or a concurrent combination of the two.

- In addition, CRT will continue work supported by the NASA MEMS program that began 3 years ago and focus on implementing an edge recognition capability in the CARES program. At the present time the CARES interface to ANSYS, entitled ANSCARES, will recognize and compute edge stresses for a handful of ANSYS elements. However, the algorithm to compute a probability failure due to edge defects for a component is missing from within CARES. CRT will consult with researchers at ORNL to ascertain which elements should be included from the ANSYS library of elements in the ANSCARES interface. Then CRT will begin the process of updating the CARES code to compute a component probability of failure due to edge defects.

- Create a capability in *CARES* to estimate "allowable" effective stress in a component when a specific failure probability is known or desired, and calculate effective stress "ranges" about the desired effective allowable stress value that are associated with any desired confidence level.

- Update *CARES* so that it interfaces with *ANSYS 8.0.*

- Create a capability to pool censored data (for the most common test specimen geometries and for user-specified loading factors or effective-areas or effective-volumes).

- Create a capability to determine confidence bounds about pooled censored data.

- Create a capability to determine confidence bounds about predicted reliability of a component.

- Create a capability to determine confidence bounds about predicted reliability of a proof-tested component.

- Update interfaces between *WeibPar* and *CARES*.

Highlights

Connecticut Reserve Technologies, LLC (CRT) is currently developing and enhancing a method to determine Weibull distribution metrics for the Ingersol Rand microturbine rotor. The combination of service stress state and a requisite probability of survival for a Si_3N_4 microturbine rotor are being used to determine Weibull modulus - characteristic strength pairs for any arbitrary Si_3N_4 scaled to standard mechanical test coupons and test methods.

CRT has also developed the ability to compute effective area, effective volumes, and reliability prediction confidence bounds using the *CARES* algorithm and the *WeibPar* software for arbitrary component geometries.

Technical Progress

The finite element model of the IR rotor originally provided to CRT had the surface geometry removed at some point in the creation of the model. CRT has modified an ANSYS macro designed to extract surface information (stress states and geometry) for elements that were attached to areas created in the solid modeling phase. The original rotor is depicted in Figure 1.

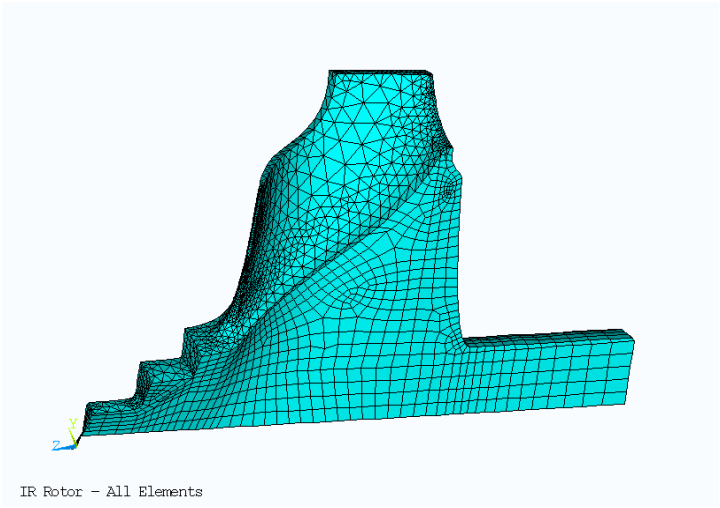

Figure 1 Entire mesh - Ingersoll Rand rotor

In extensively modifying an existing surface macro CRT was able to identify elements from within the mesh that have an element surface coincident with the surface of the rotor. These selected elements are depicted in Figure 2. Note that for elements with surfaces coincident with the surface of the rotor the entire element is shown, not just the face of the element coincident with the surface of the rotor.

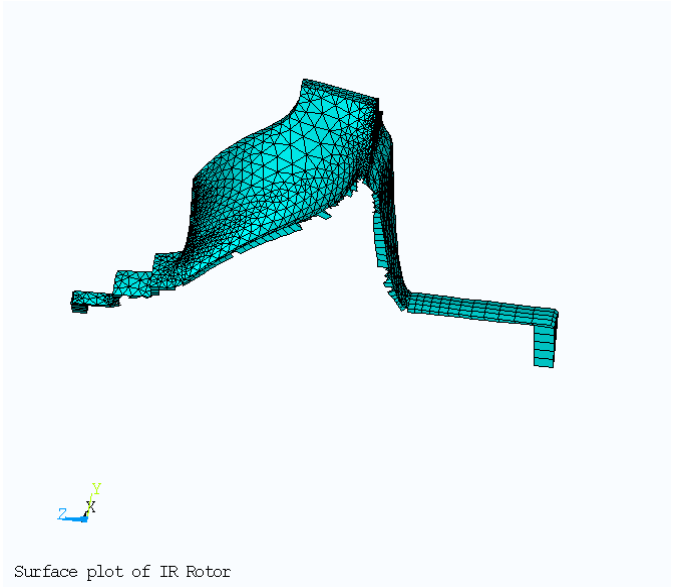

Figure 2 Elements with surfaces coincident with the surface of the IR rotos

With this information CRT can now generate Weibull metrics relative to a surface flaw analysis. The results of this endeavor will be reported on in an upcoming quarterly report.

As indicated above CRT has developed an ability to compute bounds on component reliability using bootstrap techniques. In an upcoming report CRT will provide figures similar to those depicted in Figures 3 and 4 relative to the IR rotor. In Figure 3 a relationship has been established between the effective area of a component and the Weibull modulus of the material used to fabricate the component.

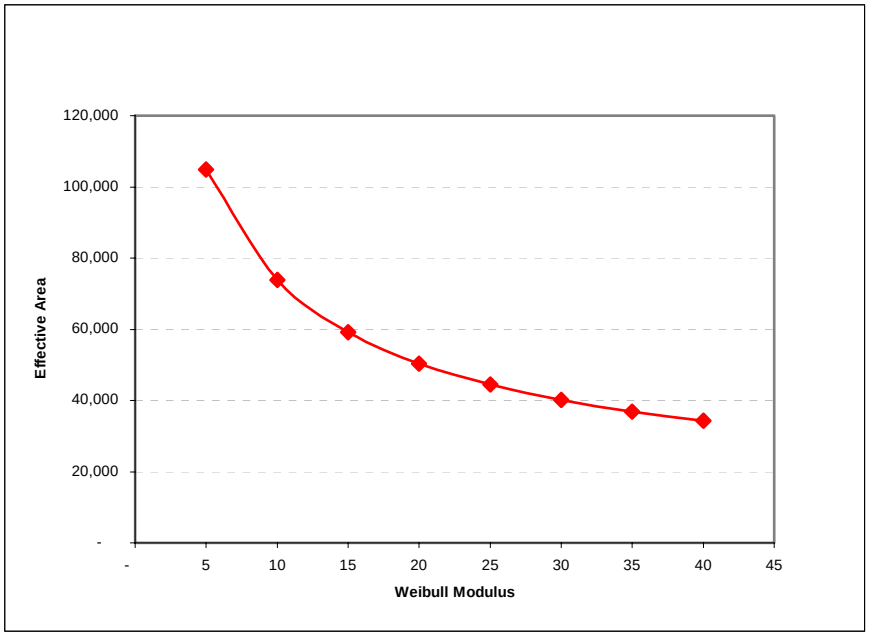

Figure 3 – Component effective area as a function of Weibull modulus

Figure 4 depicts the bounds on component reliability based on the size of the data set used to generate the Weibull parameters and the information if Figure 3. The blue diamond is the component probability of failure given the biased maximum likelihood Weibull parameters. The extreme two data points (circles) are the 5% and 95% confidence bounds. One is 90% certain that the actual component reliability falls between these two points. The open circle is the mean probability of failure. This point is the unbiased probability of failure.

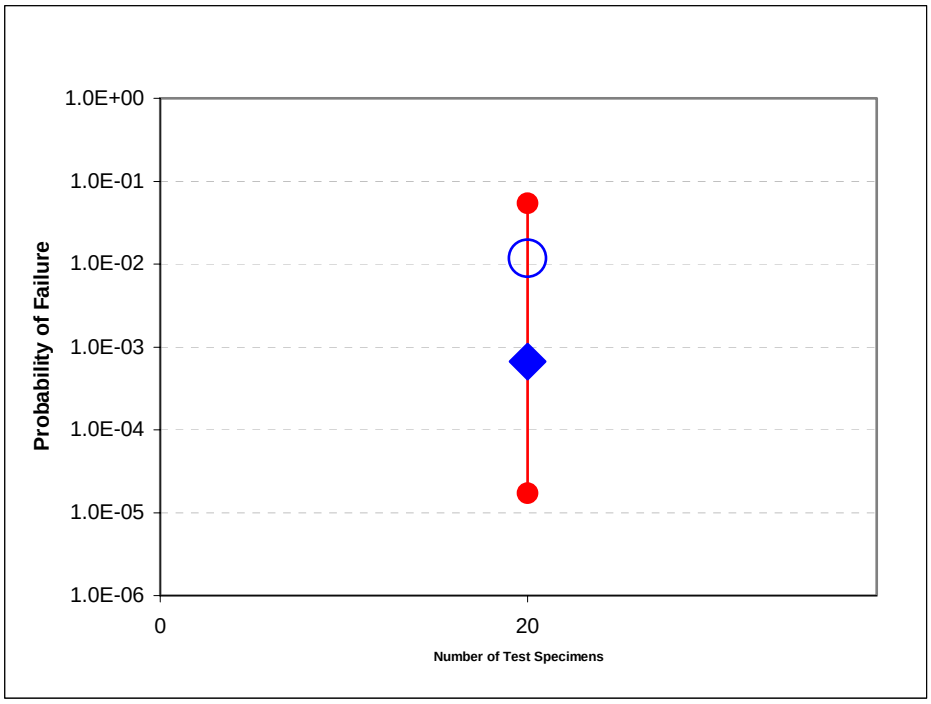

Figure 4 – Confidence bounds on component reliability

Status of Milestones

Determine characteristic strength - Weibull modulus "maps" for both surface- and volume-based flaws that limit strength in ASTM C1161B and ASTM C1161C bend bars and ASTM C1273 Button-head tensile specimen geometries. Use the stress state of the Ingersol-Rand rotor to direct those calculations and compose and submit a publication-ready ORNL/TM Report summarizing those methods and results. [30Sep04] *On schedule.*

Provide ORNL with latest versions of CARES and WeibPar. [30Sep04] *On schedule*

Industry and Research Interactions

None this reporting period.

Publications

None this reporting period

Conference Presentations

"Life Prediction of Structural Components," **S. F. Duffy**, LA Janosik, A. A. Wereszczak, B. Schenk, A. Suzuki, J. Lamon, and D. J. Thomas, Presented at the 28th Annual Cocoa Beach Conference and Exposition on Advanced Ceramics and Composites Ceramics & Components in Energy Conversion Systems Symposium Session: "Ceramic Materials and Component Characterization for Gas Turbines," January 28, 2004

NDE Technology Development for Microturbines

W. A. Ellingson, R. Visher, C. Deemer, E. R. Koehl, and Z. Metzger
Argonne National Laboratory
9700 South Cass Avenue
Argonne, IL 60439
Phone: (630) 252-5058, E-mail: Ellingson@anl.gov

Objective

The objective of this project is development of low-cost, reliable nondestructive evaluation/characterization (NDE/C) technologies for: (1) evaluating low-cost monolithic ceramics for hot section components of microturbines or industrial gas turbines, (2) evaluating environmental barrier coatings (EBCs) for monolithic ceramics and ceramic matrix composites, and (3) evaluating other materials which are part of the technology to advance the programs for the Office of Distributed Energy. The project is directly coupled to other Office of Distributed Energy projects focused on materials developments.

Highlights

There are two highlights this period. First, we more fully explored the use of the Optical Coherence Tomography (OCT) system for characterizing EBCs and second, we successfully completed the addition of more nodes, now up to 44 nodes, to the Beowolf cluster for high speed X-ray computed tomographic (CT) image reconstruction .

Technical progress

Technical work this period focused on 3 areas: (1) developments towards volumetric, 3D, X-ray imaging for improving the reliability and processing methods of low-cost monolithic ceramic materials, (2) work on oxide-based ceramic composites, and (3) work to establish characteristics of new EBCs.

Characterization of EBCs using Optical Coherence Tomography(OCT)

Work this period on OCT has focused in two areas. The first is continuing to understand the theory behind the technique so as to better apply it to EBC materials. Second, efforts have continued to improve the OCT system itself.

Volumetric Visualization of Flaws in Ceramic Rotors
High Speed Image Reconstructions using the Beowulf Computer cluster

The advances in the area of large area, high resolution flat panel X-ray detectors has enabled X-ray computed tomography (CT) to detect features much smaller in real components then were previously possible. However, the lager size and high resolution of these detectors, such as the RID 1620 detector (17" square with a 200 μm Pixel size) used at ANL, causes the time for data reconstruction to increase dramatically. The number of calculation required to compute a CT reconstruction is on the order of magnitude of N^3, where N is the number of columns in the data set. For the RID 1620, the floating point operations (FLOPs) required for reconstruction is on

the order of 100 GigaFLOPs. For a detector with half the resolution, only 10 GigaFLOPs would be required.

In a cooperative effort with the Basic Sciences Division-Materials (BSD-M) at ANL, a massively parallelized computer architecture (called a Beowulf cluster) has been developed. Using computer code developed at ANL, this cluster is capable of significantly reducing the time required for CT data reconstruction. The cluster has been specifically designed for very high speed 3D X-ray image reconstructions using the massive data sets that are being collected from the large area flat panel X-ray detectors (as large as 22 GB for a single data set on the RID 1620).

In its current configuration, the cluster the cluster contains 17 PIII 450 MHz Intel processors and three P4 2.2 GHz Intel processors. A benchmark on the reconstruction code was obtained using a typical data set. Figure 1 shows the reconstruction time as a function of the number of processors (i.e. nodes) used to perform

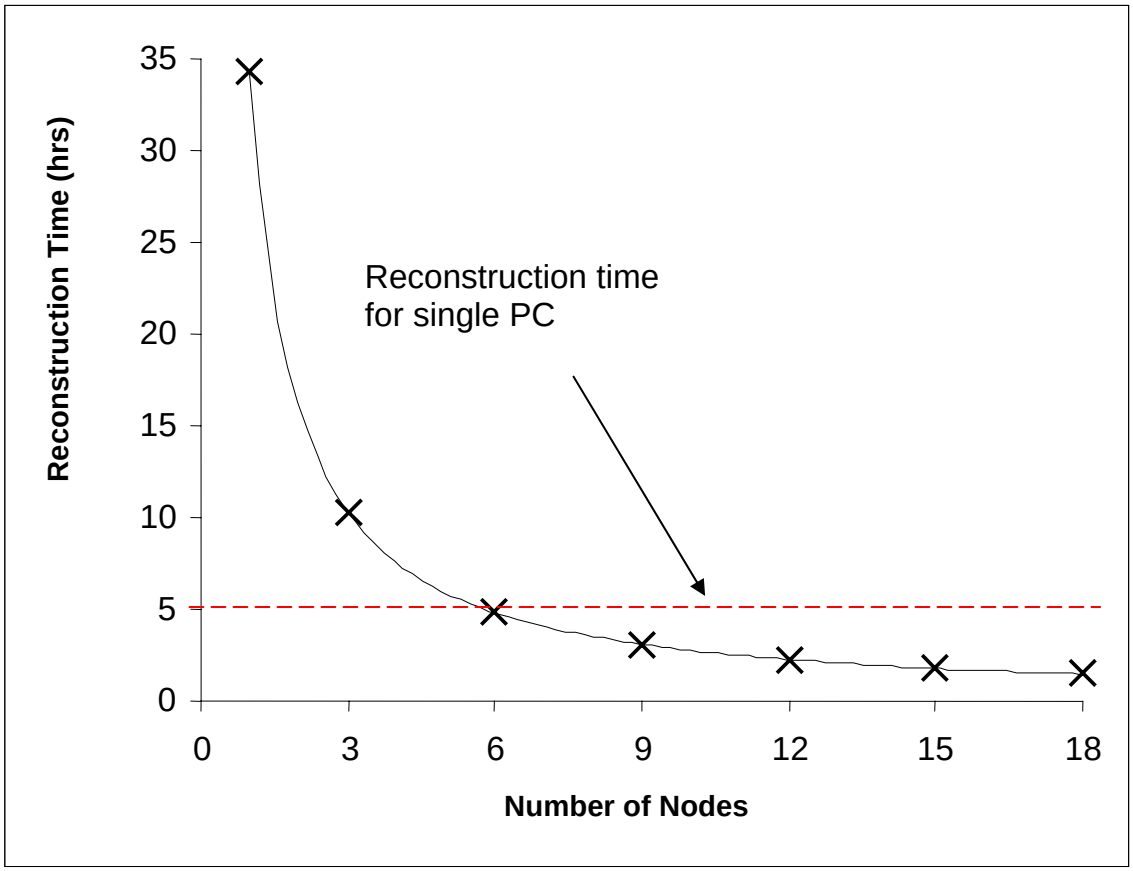

Figure 1: Plot showing the Beowulf reconstruction benchmark

the calculations. As indicated by the red line in Figure 1, a single PC workstation using dual Intel Xeon processors performs the reconstruction in approximately 5 hours. Using 18 nodes, the Beowulf cluster performs this same reconstruction in 3.5 hours, a 30 % reduction in computational time. It is important to note that the reconstruction code has yet to be optimized. Thus, the reconstruction time can be further reduced.

We added new nodes to bring the cluster up to 44 nodes and plans now are to go to 50. After the addition of each new node, the amount of savings in reconstruction time is observed. These new nodes will be based on the Intel Pentium 4 (P4) processor and have 512 MB of memory each. Once the new nodes have been added, the original 18 nodes will be upgraded to match the specifications of the new nodes. Currently, the first 3 new nodes have been added to the cluster. A "new" node (using the Intel P4 processor) can perform approximately 3 times the number of calculations than an "old" node (using the Intel PIII processor). The original cluster benchmark was performed with these additional nodes, and the calculation time was reduced by a factor of 2 when using all 21 nodes as compared to the original 18. The new benchmark curve is shown in Figure 2. It is expected, that the cluster will contain 50 P4 2.2 GHz processors by July of 2004.

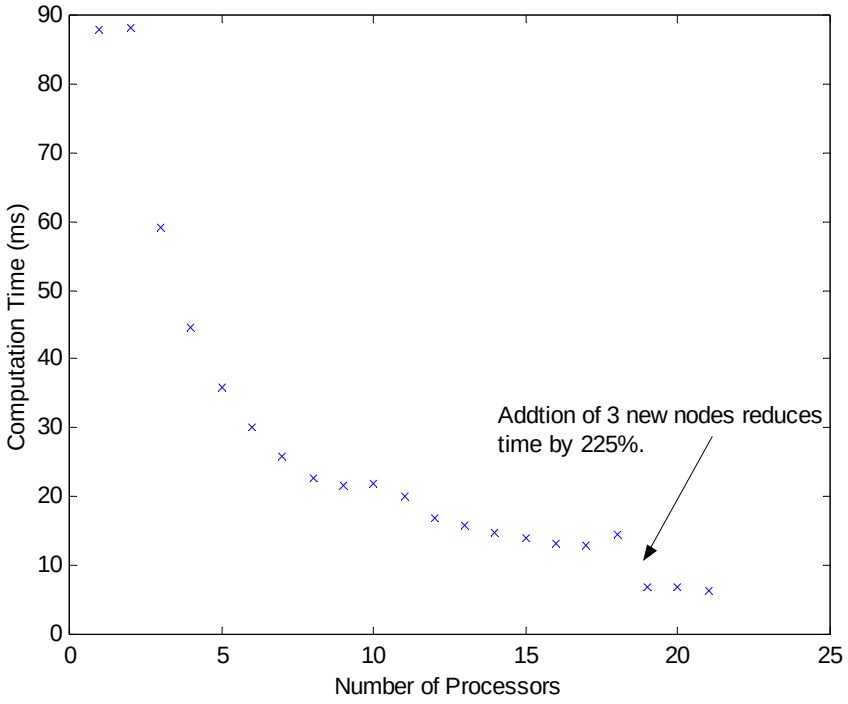

Figure 2: Beowulf cluster performance benchmark—Pi calculation.

To further investigate the capabilities of detection of flaws in monolithis ceramic mocroturbine components using new detectors, the gelcast Si_3N_4 AS800 rotor used previously was again used (see Fig 3). To again note the details, the three sections cut from the unbladed rotor had diameters of 67 mm, 112 mm, and 178 mm respectively. A series of three flat-bottom holes (having diameters of 0.4 mm, 0.6 mm, and 1.5 mm) were machined into each section using an ultrasonic drilling system. This time the detection study was done using the 450 kVp X-ray source (see 3rd Microturbine quarterly report from 2003) and two X-ray detectors were utilized; (1) an amorphous silicon flat panel area detector with a spatial resolution of 400 μm/ pixel, and (2) a linear CMOS based detector with a spatial resolution of 83 μm/ pixel. An example of a X-ray CT reconstruction from the CMOS linear detector is shown in Fig. 4. To quantify the detectability of the seeded defects using the two detectors, the relative 16-bit grey level from in the flat-bottom holes were compared to an undamaged region from each reconstruction. The grey scale difference was plotted and is shown in Fig. 5 for each flaw in each of the three sections. It is apparent that the flaw detectability of data from the high resolution CMOS detector is much better than the lower resolution area detector. It should be noted that the

RID1620 detector with 400 µm pixels could not resolve the 0.4 mm diameter hole in the 178 mm diameter section, but the CMOS detector was able to resolve this easily with a 7000 grey scale difference in the 16-bit image.

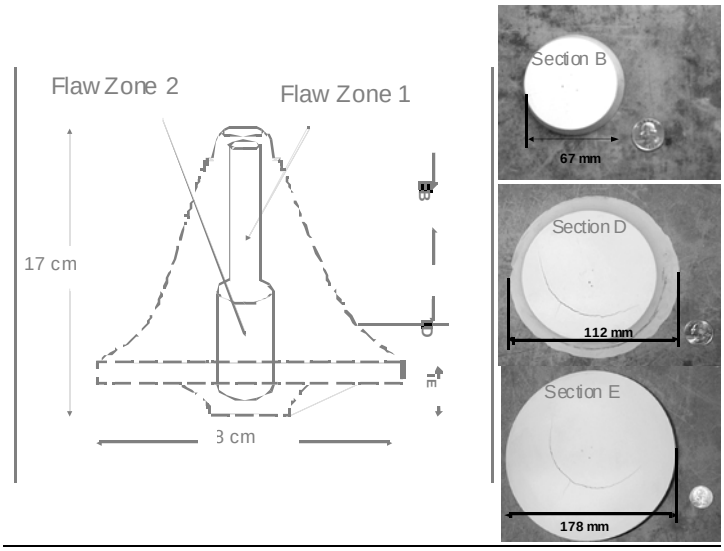

Fig. 3. Schematic diagram of unbladed gelcast AS800 microturbine rotor showing location of sections and digital photographs showing the seeded defects in sections.

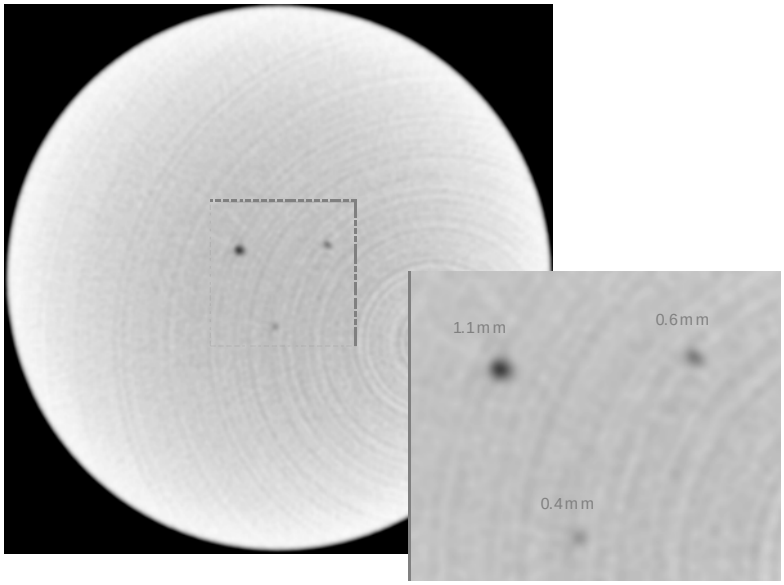

Fig. 4. CT reconstruction of the 67 mm diameter section showing the three seeded defects.

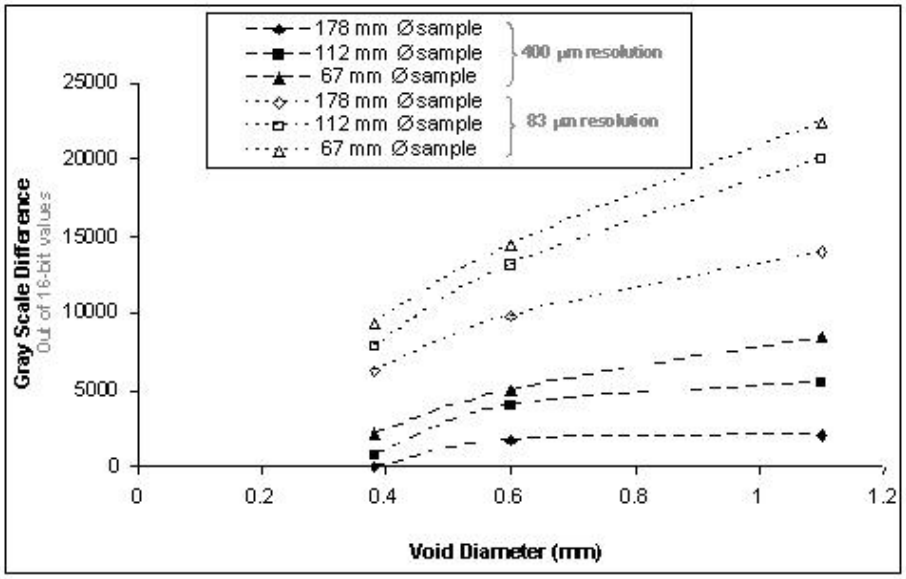

Fig. 5. Plot showing the resolution of the two detectors to identify the seeded defects

Status of milestones

A. Demonstrate high-speed 3D-X-ray computed tomography to detect critical sized flaws in full-sized monolithic rotors. The new CMOS 80µm detector has allowed detection of necessary flaws. However, speed of reconstruction for 3D volumes is still too slow and work is progressing with the Beowolf Cluster.

B. Complete installation of software for modeling laser scatter and demonstrate the ability to predict sensitivity of detection in EBCs. The software, Emflex, was installed on a Sun Blade 100 computer. The "field-solver" software, EMFlex, is now running and parameteric variables are now being added. The first reflection mode data set has been run. This allows comparison between the experiments and theory.

Industry/National Lab Interactions

1. Discussions took place with staff from Saint-Gobain Industrial Ceramics and Plastics as it was Saint-Gobain who provided the OCT system.
2. Discussions continued with staff of Solar Turbines , Siemens-Westinghouse and COI relative to oxide/oxide composites
3. Discussions also continued with staff of Northwestern University relative to EBCs for monolithic materials

Problems encountered/resolved

The RID1620 large area x-ray detector has now been returned to service and is working well after repair and modification. We have also now have excellent results with the new large length, 36-inches, CMOS linear array detector. The RID1620, with 200um square pixels, had to be returned to PerkinElmer for repair.

Trips/meetings

1. W.A. Ellingson attended the 28th International Cocoa Beach Conference and Exposition on Advanced Ceramics and Composites held January 25-30, 2004 in Cocoa Beach, FL.

2. C. Deemer attended the 28th International Cocoa Beach Conference and Exposition on Advanced Ceramics and Composites held January 25-30, 2004 in Cocoa Beach, FL. He gave a paper titled "Improved Reliability of High-Temperature Ceramic Microturbine Components through High-Speed X-ray Computed Tomography."

3. R. Visher attended the 28th International Cocoa Beach Conference and Exposition on Advanced Ceramics and Composites to be held January 25-30, 2004 in Cocoa Beach, FL. He presented a paper titled "Initial Investigation of Optical Coherence Tomography for Nondestructive Evaluation of Ceramic Coatings."

4. W. A. Ellingson plans to attend the International Gas Turbine Conference to be held in Vienna, Austria, June 13-17, 2004. He will present a paper titled" Optical Coherence Tomography as a Nondestructive Evaluation method for Ceramic Coatings."

CHARACTERIZATION OF ADVANCED CERAMICS FOR INDUSTRIAL GAS TURBINE/ MICROTURBINE APPLICATIONS

Mechanical Characterization of Monolithic Silicon Nitride Si_3N_4

R. R. Wills and S. Goodrich
University of Dayton Research Institute
300 College Park, KL-165, Dayton, OH 45469-0162
Phone: (927) 229-4341, E-mail: roger.wills@udri.udayton.edu

Objective

The objective of this project is to work closely with microturbine materials suppliers to characterize monolithic ceramics and provide the data obtained to microturbine manufacturers via a website database. User-friendly software, that will allow prospective users to readily compare different silicon nitrides, will also be developed. This project consists of the following four tasks.

Task 1: Evaluate Strength and Mechanical Properties of New Materials

This task is motivated by the materials needs of the microturbine manufacturers and the ceramic component suppliers. Consequently, Task 1 will focus on the generation of key mechanical property data for these materials with emphasis on strength, strength distribution, time-dependent failure, elastic properties, and fracture toughness. In particular, the effects of water vapor are very important.

Continued testing and evaluation of SN281/282 at 1400°C will be conducted by dynamic stressing and creep in air and water vapor. Baseline mechanical property data will also be measured for materials supplied by Kennametal and Saint Gobain Advanced Ceramics as part of their materials development effort funded by ORNL. The initial focus will be on measuring creep flexure strength. For new materials and EBC systems the focus will be on determining other properties such as thermal expansion, thermal diffusivity, hardness, elastic modulus and fracture toughness. This type of data is needed to support finite elements analyses.

Task 2: Develop "User Friendly" Software for Searching Existing Mechanical Properties Database

UDRI has received a number of requests from microturbine manufacturers for strength and time-dependent mechanical property data for current silicon nitride and silicon carbide ceramics. The current database contains a number of searchable PDF files and an Excel database containing the individual strength and creep data points by material for different temperatures. Integration of the site, with the National Aeronautics and Space Administration (NASA) Glenn's Ceramics Analysis and Reliability Evaluation of Structures (CARES)/Life software, will allow the user to predict reliability and life of various advanced ceramic materials. This tool will aid designers in their search for application-appropriate advanced ceramic materials.

The CARES computer code has a specific input format, but the existing data format used in the website is not compatible with this format. This task will focus on generating these input files for all the existing data and for data generated on new materials. In addition, the website will be redesigned and given a new URL to facilitate easier access.

Task 3: Screening of Novel Oxidation Resistant and EBC Compatible Silicon Based Ceramics

Above 1100°C, the long-term reliability of structural ceramic components is limited by loss of material through water vapor enhancing the corrosion of silicon based structural ceramics. This has necessitated the development of multilayer environmental barrier coatings (EBCs) to protect the underlying structural ceramic. In this task, UDRI will screen potential new EBC coating materials such as the aluminum silicon carbides for which no or little data currently exists. The primary screening test will be oxidation in water vapor. For new materials and EBC systems, focus will also be on determining other properties such as thermal expansion, thermal diffusivity, hardness, elastic modulus and fracture toughness, which are needed to support design work using finite element analyses.

A second approach to solving this problem is not to coat the silicon nitride but to fabricate composite silicon nitrides that contain 10-30 mol % of an oxidation resistant second phase. Studies on silicon nitride-barium aluminosilicate ceramics have shown that good mechanical properties can be obtained despite the relatively high amount of second phase. This task will concentrate on the preparation and characterization of two-phase silicon nitrides containing alkali aluminosilicates. Emphasis will be on determining the oxidation behaviour of such composites in water vapor.

Task 4: Mechanical Properties and Failure Mechanisms of EBC Coated Materials

In this task, UDRI will use its capabilities and expertise to examine the mechanical properties of EBC coated structural ceramics to determine the adhesion and reliability of the coating under load at elevated temperature.

Highlights

Dynamic fatigue testing of Kyocera's SN281 silicon nitride at 1400 and 1500°C in saturated water vapor gave slow crack growth exponents of 61 and 43, both values being higher than found in an air environment. Oxidation of aluminum silicon carbide in air at 1500°C obeyed parabolic kinetics with a dual oxide layer being formed. The database website has been modified with input files for the CARES computer design code. Files for AS-800, SN88, NT154 and GS44, and GN-10 silicon nitrides have been added.

Technical Progress

Dynamic Fatigue of Kyocera SN-281 Silicon Nitride in Air /Water Vapor Atmosphere

A water generating system was set up to flow water vapor saturated air as the atmosphere around each specimen undergoing dynamic fatigue testing at 1400 and 1500°C. The system consisted of an air pump, a flowmeter, several water bubblers contained in a constant temperature water bath, and a hygrometer immediately before the furnace. The stainless steel tubing carrying the air/water vapor mixture to the furnace was heated to 150°C to prevent condensation of water prior to it entering the furnace surrounding the test specimen. The hygrometer reading was 60°C.

Dynamic fatigue testing at 1400 and 1500°C was conducted using stressing rates of 0.003 and 30 MPa/s. While fracture origins are frequently difficult to discern in this grade of silicon nitride, it appeared that fracture occurred at surface flaws based upon optical and scanning electron microscopy. Figures 1 and 2 compare the slow crack growth behaviour at 1400 and 1500°C in both ambient air and the air /water vapor atmosphere. All the graphs were calculated using regression analysis.

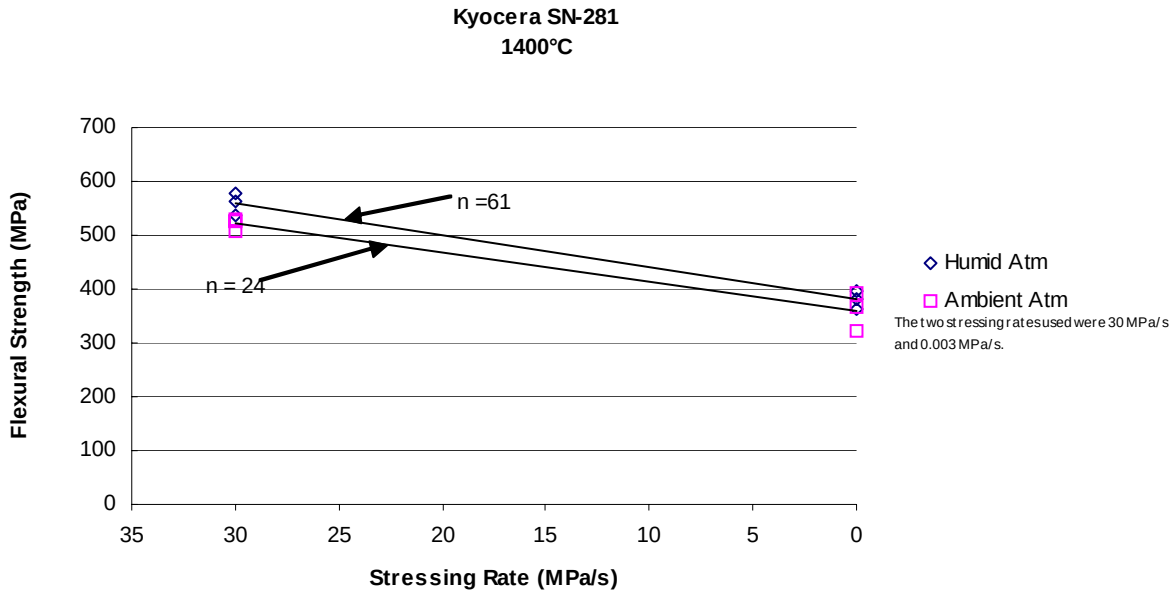

Figure 1. Dynamic Fatigue of SN281 in Air and Air/Water Vapor Atmospheres at 1400°C.

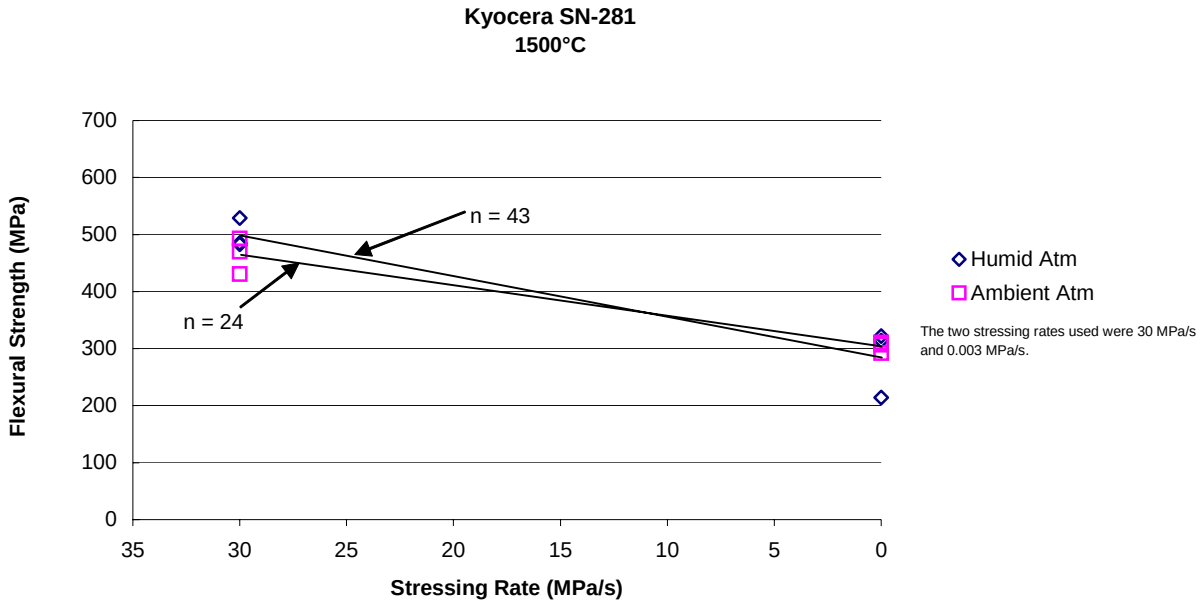

Figure 2. Dynamic Fatigue of SN281 in Air and Air/Water Vapor Atmospheres at 1500°C.

While the crack growth rates in air are identical (N=24) the addition of water vapor to the atmosphere reduces crack growth rates. This is consistent with a crack blunting mechanism due to oxidation of the silicon nitride during dynamic fatigue. Higher oxidation rates at the higher temperature in the air/water vapor atmosphere would also be expected to increase the crack growth exponent, but this is not what is observed. Rather the exponent dropped from 61 at 1400°C to 43 at 1500°C. In a water vapor saturated environment, the two principal chemical reactions occurring at the crack tip are oxidation of the silicon nitride to silica and volatilization of tetrahydroxysilane. One possible explanation for the change in slow crack growth exponent is that volatilization of material in front of the crack tip is occurring and that this is a more influential factor than oxide growth in governing crack tip velocity. Removal of local material in and around the crack tip would certainly enhance crack velocity.

Most silicon nitrides exhibit crack growth exponents in air that decrease with increasing temperature. For example, NT164 has n values of 159, 35 and 18 at 1038, 1150 and 1350°C. In contrast, SN 281 has a constant n of 24 in air at both 1400 and 1500°C. The classic explanation of slow crack growth invokes crack formation ahead of the main crack as a result of grain boundary sliding facilitated by a viscous grain boundary phase. Since the viscosity of the grain boundary phase decreases with increasing temperature, the value of n decreases. This mechanism does not appear to be operating in the SN281 silicon nitride. Rather, there appears to be some threshold based mechanism since an increase in temperature does not cause enhanced slow crack growth. Damping studies by Pezzotti, et al.[(1)] show that the lutetium silicate phases entrapped at multiple grain junctions lock grain motion and retard grain boundary sliding in this temperature regime. Grain boundary sliding and diffusional flow do not occur until >1620°C.

The most likely model to explain the above data would be one that assumes that a crack propagates along the grain boundary by a process of surface and grain boundary diffusion in which adjoining grains behave elastically. Chang[2] developed such a model and showed good agreement between theory and experiment with a set of creep crack growth data on several Si-Al-O-N samples.[3] In this model:

$$K/K_{min} = 1/2[(v/v_{min})^{1/2} + (v/v_{min})^{-1/2}] \quad (1)$$

where K is the stress intensity factor, $K_{min} = 1.69\ K_{ic}$ is the minimum K below which no crack growth is predicted, K_{ic} is the critical stress intensity factor, v is the crack tip velocity , and v_{min} is the minimum crack velocity for $K=K_{min}$.

It seems likely that slow crack growth in SN281 follows this model.

Upgrading the Website

The website has been modified so that users can see that CARES input files are being added to the site. Files for AS-800, SN88, NT154 and GS44, and GN-10 silicon nitrides have been added. These files include test conditions, specimen geometry, surface finish and failure stresses. The modified website can be viewed at http://www.udri.udayton.edu/design_data_files.

Aluminum Silicon Carbides: a Potential EBC

Aluminum containing ceramics generally possess good oxidation resistance and are thus worthy of consideration as EBCs. While many of these have been considered or are currently under investigation as potential EBCs, one group of aluminum containing ceramics that has received little attention to date is the aluminum silicon carbides. Although little property data exists for these materials, initial oxidation studies on Al_4SiC_4[4] indicate the formation of a thin protective oxide layer of alumina and mullite. The objective of the current task is to determine the oxidation resistance of these materials in water vapor and to determine some of their basic properties and, hence, ascertain whether or not these materials can be considered as viable EBC materials.

Small rectangular plates approximately 0.6 in x 0.3 in x 0.04 in were cut out of the hot pressed billet. After cleaning, the Al_4SiC_4 was subjected to oxidation at 1500°C in air. An initial sample was oxidized for 48 hours, and the oxidation kinetics were determined over 144 hours in air by weighing the sample at several intervals.

The data was examined for linear, parabolic and logarithmic kinetics. Excellent correlation with parabolic kinetics (see Figure 3) was found. This form of oxidation kinetics is also typically exhibited by silicon carbide and silicon nitride ceramics. Both samples showed two layers covering the Al_4SiC_4. Figure 4 shows these two layers formed after oxidation at 1500°C for 144 hours. The outer surface was rough and porous, as shown in Figure 5, and not what one would like to see for a protective oxide.

After 48 hours, the thicknesses of the inner and outer layer were 60 and 40 microns. After 144 hours, the inner layer is largely unchanged in thickness but the outer layer had grown to 75 microns. Based upon x-ray diffraction analysis and elemental mapping, the outer oxide layer is mainly alumina with some mullite and the inner layer a mullite layer. The difference in thermal expansion of these materials explains the delamination seen between these layers in some of the micrographs. The alumina grains are blocky and approximately 10 microns in size, whereas some acicular grains can be seen in the inner mullite layer.

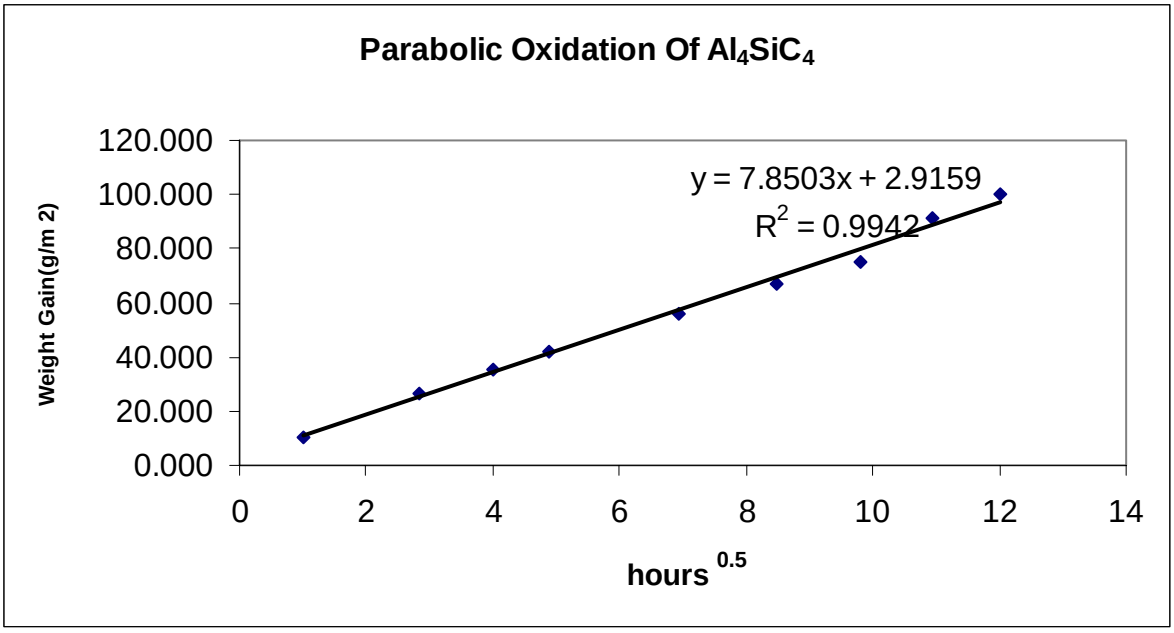

Figure 3. Parabolic Oxidation Kinetics of Al_4SiC_4 in Air at 1500°C.

Al_4SiC_4 Layer 1 Layer 2

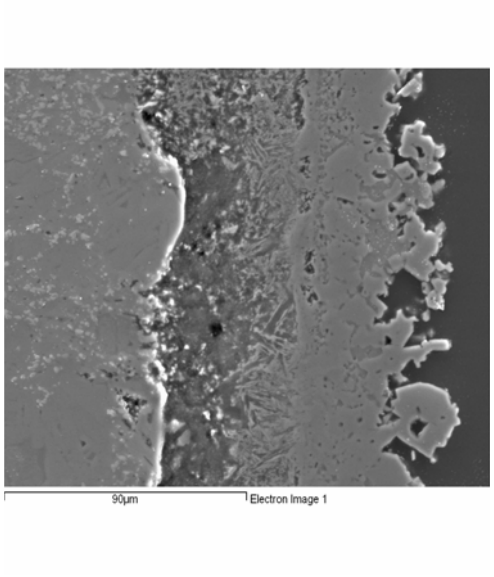

(a)

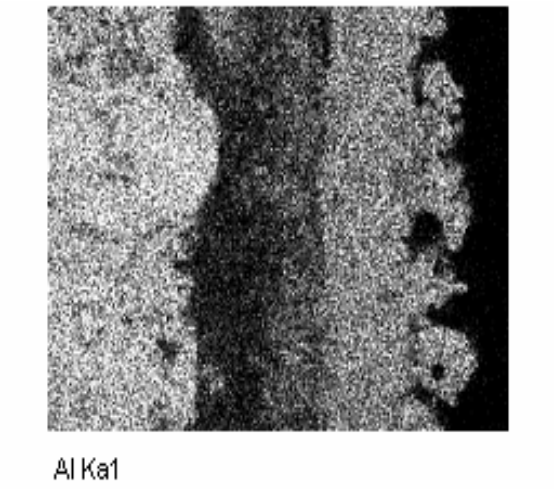

(b)

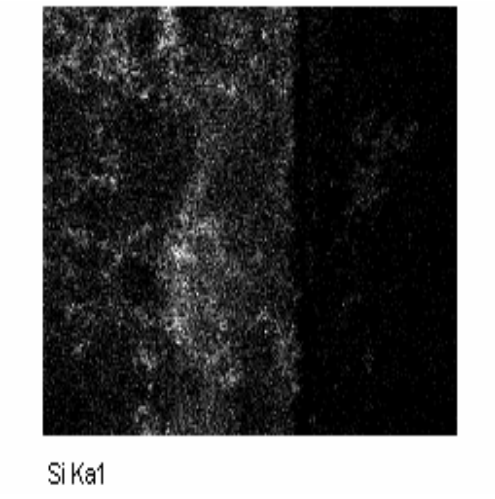

(c)

Figure 4. Cross Section of Two Surface Oxide Layers on Al_4SiC_4. (a) On the Al_4SiC_4 after exposure to air at 1500°C for 144 hours together with aluminum (b) and silicon (c) EDAX scans.

(Note: the inner oxide layer contains much less aluminum than either the substrate or the outer oxide layer.)

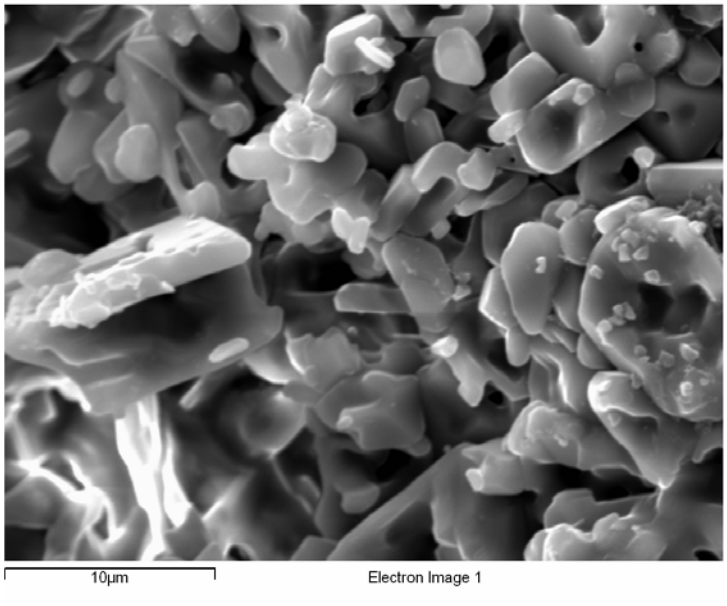

Figure 5. Microstructure of Surface Oxide Layer Showing Internal Porosity.

Status of Milestones

1) Testing and Evaluation of SN-281/282

Slow crack growth testing in both air and air/water vapor at 1400 and 1500°C has been completed.

2) Testing of Materials from Kennametal and St. Gobain

Heat capacity of NT154 has been completed.

3) Evaluation of Aluminum Silicon Carbide

Sample preparation and oxidation in air has been completed. Oxidation kinetics in water vapor and thermal properties need to be completed.

Industry and Research Interactions

A visit was made to Oak Ridge National Laboratory and a presentation given. A brief discussion was held with John Holowczak and Ellen Sun regarding oxidation of BSAS. One ORNL paper was reviewed.

Problems Encountered

None

Publications

None

References

1. G. Pezzotti, K. Ota, Y. Yamamoto, and Hua-Tay Lin, "Elementary Mechanisms behind the High Temperature Deformation Behaviour of Lutetium Doped Silicon Nitride," *J. Amer. Ceram. Soc.* 86(3), 471(2003).

2. T. Chang, "A Diffusive Crack Growth Model for Creep Fracture," *J. Amer. Ceram. Soc.* 65(2), 93 (1982).

3. M.H. Lewis and B.S.B. Karunaratne, "Determination of High Temperature K_1 –V Data for Si-Al-O-N Ceramics," pp 13-32 in Fracture Mechanics Methods for Ceramics, Rocks and Concrete. Edited by S.W. Freiman and E.R. Fuller, Jr., ASTM STP 745 (1981).

4. J. Schoennahl, B. Willer, and M. Daire, "Preparation and Properties of Sintered Materials in the Systems Si-Al-C and Si-Ti-C," p. 338 in Materials Science Monographs 4: Sintering- New Developments, Elsevier Science Publishing, Amsterdam (1979).

Microstructural Characterization of CFCCs and Protective Coatings

K. L. More and P. F. Tortorelli
Metals and Ceramics Division
Oak Ridge National Laboratory
Oak Ridge, Tennessee 37831-6064
Phone: (865) 574-7788, E-mail: koz@ornl.gov

Objectives

Characterization of CFCC materials and CFCC combustor liners after exposure to simulated (ORNL's Keiser Rig) and actual (engine tests) combustion environments

Exposures of candidate environmental barrier coatings (EBCs) to high water-vapor pressures (in Keiser Rig) to determine thermal stability and protective capability

Work with CFCC and coating suppliers/manufacturers to evaluate new/improved ceramic fibers, protective coatings, and composite materials

Highlights

During this quarter, a meeting was held at Solar Turbines on March 31 to determine an evaluation plan for two sets of CFCC/EBC combustor liners which were exposed at either the Chevron and Malden Mills engine test sites. Research staff from ORNL, UTRC, and Solar Turbines attended the meeting.

Technical Progress

Two sets of CFCC/EBC combustor liners have recently been removed from engine tests (conducted by Solar Turbines) and will be evaluated microstructurally and mechanically at ORNL. Details of the CFCC/EBC combustor liners and engine test conditions are as follows:

Chevron Test #6

Inner Liner –Hi-Nicalon fiber, melt-infiltrated (MI) SiC/SiC liner with a Si/BSAS EBC (no intermediate layer) – produced by Goodrich, Inc.

Outer Liner – enhanced SiC/SiC (CVI) liner with a Si/(Mullite+BSAS)/BSAS EBC – produced by GE Power Systems Composites

Inner liner ran for 5,135 hours, 43 starts. Outer liner was first refurbished liner that ran initially for 7,238 h, was refurbished, and ran an additional 5,135 h in Chevron Test #6. Only inner liner will be evaluated at ORNL (outer liner may be refurbished again for additional engine testing).

Malden Mills #3

Inner Liner – Tyranno fiber, MI SiC/SiC liner with a Si/SAS EBC – produced by GE Power Systems Composites

Outer Liner – Tyranno fiber, MI SiC/SiC liner with a Si/(Mullite+SAS)/SAS EBC – produced by GE Power Systems Composites

Inner and outer liner set ran for a total of 8,368 h and 32 starts (engine #2) before being removed from engine test due to extensive EBC loss on inner liner. Both inner and outer liners will be evaluated at ORNL.

All three of the liners to be evaluated were bulk cut at Solar Turbines and have been received at ORNL for additional sectioning into coupons for microstructural characterization and mechanical testing. These liners will provide for several unique characterization opportunities to add to an existing and extensive database on characteristics of engine-tested CFCC/EBC combustor liners. To date, the primary focus of the engine tests and subsequent characterization has been on evaluating the current state-of-the-art BSAS-based 3-layer EBC system applied to several different CFCC liners. Previous engine tests conducted at both Chevron (test #5) and Malden Mills (tests #1 and #2) had CFCC liners with the 3-layer BSAS-based EBC. Application of this EBC system to the gas-path surfaces of the CFCC liner increased the liner lifetimes significantly, however, significant volatilization of the BSAS top-coat was observed on these coated liners. The liners to be evaluated in this new study have different EBC systems; and inner liner with only a 2-layer Si/BSAS EBC and inner and outer liners with SAS-based EBCs.

Photographs of the gas path surfaces for each of the liners described above are shown in Figures 1, 2, and 3. Figure 1 shows the inner liner with a Si/BSAS 2-layer EBC from Chevron engine test #6. Extensive loss of the EBC was observed after only 5,135 h engine testing. Figure 2 shows the surface of the inner liner from Malden Mills engine test #3 which had a Si/SAS 2-layer EBC. Nearly the entire CFCC was exposed due to loss of the EBC. The outer liner from the Malden Mills engine test #3, Figure 3, exhibited minimal EBC loss.

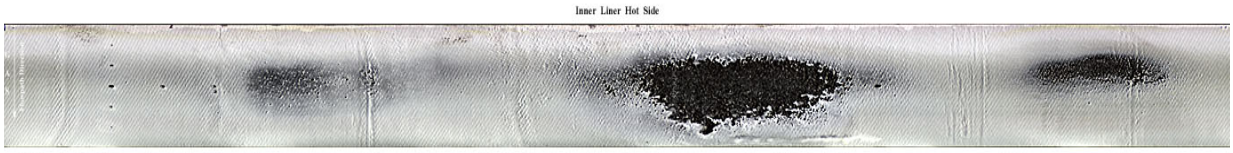

Figure 1. Gas-path surface of inner liner from Chevron engine test #6 showing localized loss of Si/BSAS EBC.

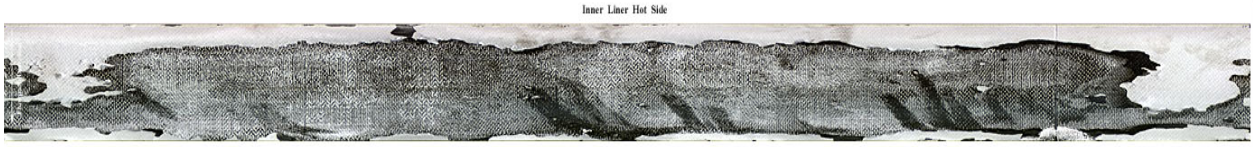

Figure 2. Gas-path surface of inner liner from Malden Mills engine test #3 showing extensive loss of Si/SAS EBC across entire surface.

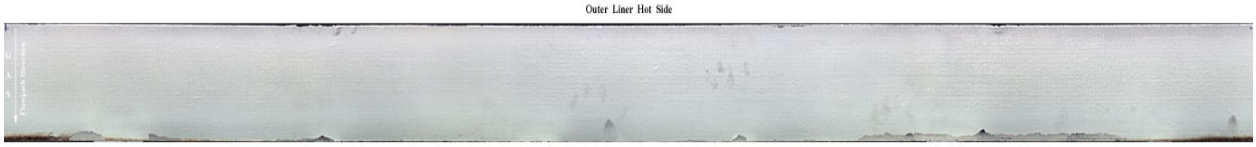

Figure 3. Gas-path surface of outer liner from Malden Mills engine test #3 showing minimal loss of Si/(Mullite+SAS)/SAS EBC.

Status of Milestones

06/04 Milestone — Prepare a report and present results on the evaluation of oxide/oxide composite materials exposed in the Keiser Rig for use as microturbine or stationary gas turbine combustor liners. (June 2004)

This milestone is in progress and will be completed on time. ATK-COI Ceramics, Inc. oxide/oxide composite material, A/N720, is currently being exposed under simulated microturbine exhaust conditions in ORNL's Keiser Rig at 1200°C for 3000 h. Results are completed for exposure of the same material for 3000 h @ 1135°C.

Industry Interactions

1. Study underway with Andy Szweda of ATK-COI Ceramics, Inc. to expose A/N720 oxide/oxide composites in the Keiser Rig at 1200°C for 3000 h in 1000 h increments. Post-exposure characterization (microstructural and mechanical) is being conducted.

2. Visited ATK-COI Ceramics, Inc. on March 30, 2004 and gave separate presentations summarizing work on (1) oxide/oxide exposures in the Keiser Rig, (2) high water-vapor pressure experiments in the Keiser Rig, and (3) microstructural evaluation of PIP-processed CFCCs.

3. Attended meeting at Solar Tubines, Inc. on March 31, 2004 (with UTRC) to discuss evaluation of CFCC/EBC combustor liners recently removed from engine tests at Chevron and Malden Mills.

4. Collaboration is ongoing with UTRC to expose BSAS, BAS, and SAS coupons and Si-based standards in the Keiser Rig at very high (~20 atm) water-vapor pressures to induce volatilization (see DE Quarterly Report for 10/03-12/03).

5. Study underway with Rishi Raj from the University of Colorado to expose candidate EBC compositions in the Keiser Rig at 1200°C and 10% H_2O. Pre- and post-exposure microstructural characterization is being conducted to evaluate stability of experimental coatings.

Problems Encountered

None

Publications/Presentations

1. P.F. Tortorelli and K.L. More, "Evaluation of EBCs in the Keiser Rig," presented at the DER EBC Workshop, Nashville, TN, Nov. 18-19, 2003.
2. K.L. More, E. Lara-Curzio, P.F. Tortorelli, A. Szweda, D. Carruthers, and M. Stewart, "Evaluating the High Temperature Stability of an Oxide/Oxide Composite Material at High Water-Vapor Pressures," presented at the 28th Annual Advanced Ceramics and Composites Conference, January 26-29, 2004, Cocoa Beach, FL.